International Journal of Biological Macromolecules 385 (2026) 155000

Contents lists available at ScienceDirect

International Journal of Biological Macromolecules

journal homepage: www.elsevier.com/locate/ijbiomac

Fermentation-associated restructuring of chickpea proteins modulates interfacial functionality and lipid-phase organization in coconut oil-based artificial fat systems☆

Jung Soo Kim [a,b,1], Jiyoon Kim [a,b,c,1], Kwang-Deog Moon [a,*]

[a] School of Food Science and Biotechnology, Kyungpook National University, 80 Daehak-ro, Daegu, 41566, Republic of Korea
[b] 3D Food Printing Technology Research Institute, FOODPRO CO., Ltd., 14 Bokhyeon-ro, Daegu, 41530, Republic of Korea
[c] Smart Food Manufacturing Research Group, Korea Food Research Institute, 245 Nongsaengmyeong-ro, Wanju-gun, 55365, Republic of Korea

ARTICLE INFO

Keywords:
Emulsifier
Structure-functional relationships
Enzymatic modification

ABSTRACT

Native pulse proteins often require structural modification to improve their functionality in artificial fat (AF) systems. This study investigated the structure–function associations between Rhizopus oryzae solid-state fermentation of chickpeas and the performance of coconut oil-based AF systems. Chickpeas were fermented for 0, 24, 48, and 72 h, and fermentation-associated differences in protein molecular profile, secondary structure, thiol–disulfide state, solubility, and surface hydrophobicity were evaluated. The resulting chickpea-derived fractions were incorporated into AF systems, which were characterized in terms of emulsion performance, rheological behavior, crystalline organization, and thermal transitions. Increasing fermentation time was accompanied by a decrease in α-helix content from 4.75% to 1.70% and an increase in β-sheet content from 27.95% to 34.25%, together with non-linear changes in thiol–disulfide balance. Among the tested conditions, 24 h fermentation provided the most favorable combination of protein solubility and surface hydrophobicity. Correspondingly, AF-24 h exhibited the highest emulsion activity index (7.75 m^2/g), greater absolute zeta potential, favorable thermal retention of apparent emulsion activity, and the strongest bulk rheological response. X-ray diffraction and differential scanning calorimetry further revealed fermentation-dependent differences in the crystalline organization and crystallization–melting behavior of the dispersed coconut oil phase. In contrast, the 72 h fermented fraction showed lower protein dispersibility and less favorable emulsion, rheological, and lipid-phase characteristics. Overall, these findings indicate that controlled *R. oryzae* fermentation can modify the functional state of chickpea-derived fractions and is associated with the structural performance of coconut oil-based AF systems, supporting their potential as plant-derived structuring components for artificial fat applications.

1. Introduction

Alternative proteins are increasingly being explored as biological macromolecules that can provide nutritional value while contributing to texture, stability, and interfacial behavior in sustainable food systems. Their performance is closely related to molecular structure, conformational flexibility, surface characteristics, and intermolecular interactions, which affect properties such as solubility, emulsification, gelation, and interfacial stabilization [1]. These structure-dependent properties are particularly important in multiphase food systems, where proteins act not only as nutrients but also as surface-active and structure-forming components.

Fat is a major structural component in meat and meat analog systems, contributing to appearance, texture, mouthfeel, flavor perception, rheological behavior, and thermal response [2]. Structured lipid phases also affect processing stability and fat distribution in meat analog products [3]. Coconut oil has been considered a useful plant-derived lipid source for animal fat alternatives because of its high saturated fatty acid content, medium-chain triacylglycerol-rich composition, and solid-like behavior near room temperature [4]. However, coconut oil

☆ This article is part of a Special issue entitled: 'Alternative Proteins' published in International Journal of Biological Macromolecules.

* Corresponding author at: College of Agriculture & Life Sciences building No. 3, Kyungpook National University, 80 Daehak-ro, Buk-gu, Daegu, Republic of Korea.
E-mail address: kdmoon@knu.ac.kr (K.-D. Moon).

[1] These authors contributed equally to this work.

https://doi.org/10.1016/j.ijbiomac.2026.155000
Received 30 June 2026; Received in revised form 6 September 2026; Accepted 21 October 2026
Available online 22 October 2026
0141-8130/© 2026 Published by Elsevier B.V.

alone has limited applicability in structured food systems because of its brittle texture, narrow melting range, and low mechanical adaptability. Stabilization with suitable macromolecules is therefore needed to improve the structural integrity and performance of coconut oil-based fat alternatives.

In this study, artificial fat (AF) systems refer to plant-derived structured emulsions designed to mimic selected structural and physical attributes of animal fat phases, rather than chemically synthesized fats. These systems require controlled droplet dispersion, interfacial stabilization, rheological structuring, and lipid crystallization behavior. The emulsifying phase is therefore central to AF formation because protein adsorption, molecular rearrangement, and intermolecular association at the oil-water interface influence droplet formation, emulsion retention, and bulk rheological properties [5].

Plant proteins are promising emulsifying and structuring agents for lipid-based food systems, but many native pulse proteins show limited interfacial activity because of their compact conformation, restricted solubility, and low exposure of surface-active groups [6]. These structural constraints can reduce protein diffusion, adsorption, and rearrangement at the oil-water interface, thereby limiting their ability to stabilize complex emulsion-based lipid systems. Structural modification is therefore often required to improve the interfacial and structuring potential of pulse proteins [6,7].

Several approaches, including enzymatic hydrolysis, ultrasound treatment, pH-shifting, and other physical or chemical modifications, have been used to alter plant protein structure and improve their technological properties [1,6]. Unlike single-enzyme or purely physical treatments, solid-state fermentation (SSF) modifies proteins within an intact food matrix, where fungal growth and multiple enzymatic reactions occur simultaneously. In particular, SSF using filamentous fungi of the genus Rhizopus induces biochemical and structural changes in legume matrices [8,9]. During fermentation, fungal enzymes such as proteases, amylases, and lipases can modify proteins, carbohydrates, and lipids within the substrate [10]. These changes may alter protein molecular profiles, expose buried functional groups, and reorganize intermolecular interactions, which can affect solubility, surface hydrophobicity, and interfacial behavior [11]. SSF therefore provides a distinct bioprocessing route for generating fermentation-modified protein fractions with potential use in structured lipid systems.

Chickpea (*Cicer arietinum* L.) is a widely consumed pulse and a promising plant protein source because of its high protein content, balanced amino acid composition, and good digestibility [12]. Its major storage proteins, mainly globulins and albumins, are associated with favorable nutritional quality and relatively low allergenic potential compared with soybean proteins [12]. Previous studies on chickpea fermentation have mainly focused on tempeh production and associated nutritional, physicochemical, biological, or general functional changes [13,14]. Our previous study developed chickpea tempeh as a texture-modified food system and showed that Rhizopus oryzae fermentation was associated with biological, physicochemical, microstructural, molecular, and textural changes in chickpea matrices [15]. However, that study was directed toward dysphagia-oriented texture design, leaving unresolved whether fermentation-associated changes in chickpea protein fractions can be translated into interfacial behavior and lipid-phase stabilization.

Most studies on fermented legume proteins have focused on conventional oil-in-water emulsions or general properties such as solubility and emulsifying activity. Much less is known about their behavior in high-oil, coconut oil-based AF systems, where droplet stabilization, rheological structuring, crystallization, and thermal transitions occur together. In addition, the relationship between multilevel protein properties and lipid-phase organization in protein-stabilized AF systems remains insufficiently understood. This gap is important because the physical behavior of structured fat alternatives can be affected not only by the lipid phase itself but also by the interfacial and network-forming characteristics of the stabilizing macromolecules.

Therefore, this study investigated structure-function associations between *R. oryzae* SSF-mediated changes in chickpea protein fractions and the behavior of coconut oil-based AF systems. Heat-treated fermented chickpea powders obtained at different fermentation times were characterized in terms of protein molecular profile, secondary structure, sulfhydryl-disulfide balance, solubility, and surface hydrophobicity. Their neutralized alkaline-extracted fractions were then incorporated into coconut oil-based AF systems, and the resulting droplet stabilization, emulsion performance, rheological behavior, crystalline organization, and thermal transition behavior were evaluated using beef tallow and coconut oil as reference systems. This study aimed to clarify how fermentation-associated differences in chickpea-derived protein fractions are linked to the interfacial and lipid-phase organization of plant protein-stabilized AF systems.

2. Materials and methods

2.1. Materials

Chickpeas (*Cicer arietinum* L.) imported from Canada were purchased from a local grocery store. Chickpeas were fermented using *R. oryzae* starter (Cultures for Health, Morrisville, NC, USA) and brown rice vinegar (Ottogi, Anyang, Korea). Coconut oil imported from Malaysia and NaCl (Chungjungone, Seoul, Korea) were purchased from a local grocery store and used to prepare AFs. Beef tallow from kidney was purchased from Daejeo (Busan, Korea) for comparison of its structural characteristics with AFs. Reagent-grade or purer chemicals used included HCl and urea (Duksan, Ansan, Korea); NaOH and glycerol (Junsei Chemical, Tokyo, Japan); EDTA (Sigma-Aldrich, St. Louis, MO, USA); sodium dodecyl sulfate (SDS), 5,5′-dithiobis-2-nitrobenzoic acid (DTNB), bicinchoninic acid (BCA), 8-anilino-1-naphthalenesulfonic acid (ANS), and bovine serum albumin (Thermo Fisher Scientific, Waltham, MA, USA); 0.5 M Tris-HCl (pH 6.8), tris, and glycine (Biosesang, Seongnam, Korea); molecular weight marker (Bio-Rad, Hercules, CA, USA); bromophenol blue (Oriental Chemical, Tai Wai, Hong Kong); and β-mercaptoethanol (β-ME; Yakuri Pure, Kyoto, Japan).

2.2. Preparation of heat-treated fermented chickpea powders

Fermented chickpeas were prepared by solid-state fermentation (SSF) using *Rhizopus oryzae* following the procedure described in our previous study with modifications. Briefly, chickpeas were washed and soaked in distilled water at a chickpea-to-water ratio of 1:3 (*w*/w) for 12 h at room temperature. The soaked chickpeas were then cooked at 95–98 °C for 30 min and cooled at room temperature for 15 min. The cooked chickpeas were coarsely ground to an average particle size of approximately 3.5 mm, mixed with brown rice vinegar, and inoculated with 1% (*w*/w) commercial *R. oryzae* starter. The inoculated chickpea mixture was portioned into perforated plastic bags at 70 g per bag and shaped to approximately 120 × 80 × 15 mm. The samples were fermented under aerobic solid-state conditions at 33 ± 2 °C for 0, 24, 48, and 72 h.

After fermentation, the samples were heated in a convection oven at 175 °C for 5 min to terminate fungal growth and standardize post-fermentation handling, followed by cooling at room temperature for 8 min. The heat-treated fermented chickpeas were freeze-dried, ground for 2 min using a grinder, and passed through a 355 μm standard sieve. The resulting powders were used for subsequent structural, functional, and artificial fat preparation experiments. Because the post-fermentation heat treatment may also influence protein conformation, aggregation, and sulfhydryl-disulfide reactions, the structural and functional results were interpreted as fermentation-associated differences in heat-treated fermented chickpea powders rather than changes caused solely by fermentation. The crude protein contents of chickpea powders, determined by the micro-Kjeldahl method, are presented in Table 1.

Table 1
Crude protein contents of chickpea powders with different fermentation times.

Fermentation time (hour)	0 h	24 h	48 h	72 h
Crude protein (%)	23.10 ± 0.14^{d}	24.96 ± 0.45^{c}	29.77 ± 0.50^{b}	34.58 ± 0.42^{a}

Values are presented as the mean ± SD ($n = 3$). Different letters within the same row indicate significant differences ($p < 0.05$).

2.3. Structural properties of chickpea protein

2.3.1. Sodium dodecyl sulfate-polyacrylamide gel electrophoresis (SDS-PAGE)

The protein molecular profiles of fermented chickpea powders were analyzed by SDS-PAGE according to a modified method from Liu et al. [9]. The gels consisted of a 5% stacking gel and a 12% separating gel, respectively. Each sample (25 mg/mL) was mixed with 5× sample buffer (40% glycerol, 10% SDS, 2% (*w/v*) bromophenol blue, and 0.5 M Tris at pH 6.8, and 20% β-ME), followed by heating at 95 °C for 10 min. Subsequently, 12 μL of each sample and 5 μL of molecular weight marker (15–245 kDa) were loaded onto the gels. Electrophoresis was performed at 150 V and 70 mA. The gels were stained and destained before image acquisition.

2.3.2. Turbidity

The turbidity of fermented chickpea powder was determined by the method of Ma et al. [16]. Each sample (100 mg/mL) was dispersed in DW, and the solution was adjusted to pH 12 using 4 M NaOH. The dispersion was stirred for 1 h and then centrifuged at 2000 ×*g* and 20 °C for 10 min. The supernatant was collected and adjusted to pH 7 using 1 M HCl. The turbidity was measured at 600 nm using a UV–Vis spectrometer (Evolution 201 UV–Visible Spectrophotometer, Thermo Fisher Scientific, Waltham, MA, USA). DW was used as the blank.

2.3.3. Circular dichroism (CD) spectroscopy

The secondary structure distribution of the soluble protein fraction from heat-treated fermented chickpea powders was evaluated by circular dichroism (CD) spectroscopy [17]. Sample dispersions were prepared at 1 mg/mL in 5 mM potassium phosphate buffer (pH 7.0), stirred for 1 h, and centrifuged at 10,000 ×*g* for 5 min at 4 °C. The supernatant was carefully collected and used for CD analysis. CD spectra were recorded using a CD spectrometer equipped with a 0.5 mm path-length quartz cell over a wavelength range of 190–260 nm at a scan rate of 100 nm/min. Buffer spectra were subtracted as the baseline, and three independently prepared samples were analyzed; each spectrum was obtained by averaging three consecutive scans.

The contents of secondary structural elements, including α-helix, β-sheet, β-turn, and random coil, were estimated using the BeStSel web server. The fitting was performed using the measured far-UV CD spectral range after baseline correction. Because the samples were prepared from chickpea powder dispersions rather than purified protein isolates, the CD results were interpreted as secondary structural estimates of the soluble protein fractions obtained under the present preparation conditions.

2.3.4. Sulfhydryl group and disulfide bond

Free sulfhydryl groups, total sulfhydryl groups, and disulfide bonds were measured using Ellman's assay with slight modifications [18]. Sample dispersions were prepared at 100 mg/mL. For free sulfhydryl determination, 1 mL of sample dispersion was mixed with 4 mL of Tris-Gly buffer A containing 86 mM Tris, 90 mM glycine, and 4 mM EDTA at pH 8.0. For total sulfhydryl determination, the same procedure was performed using buffer B, which consisted of buffer A containing 0.5% SDS and 6 M urea. Subsequently, 50 μL of Ellman's reagent, prepared by dissolving DTNB at 4 mg/mL in buffer A, was added to each mixture. The mixtures were incubated at 25 °C for 15 min in the dark, and the absorbance was measured at 412 nm. The corresponding reaction buffer was used as the blank.

The sulfhydryl content was calculated using the following equation (Eq. (1)):

$$SH\ content\ (\mu mol/g\ protein) = \frac{73.53 \times A_{412} \times D}{C \times Crude\ protein\ content} \quad (1)$$

where A_{412} is the absorbance at 412 nm, D is the dilution factor, C is the sample concentration (mg/mL), and crude protein content is the protein fraction of each fermented chickpea powder. The disulfide bond content was calculated as half of the difference between total sulfhydryl and free sulfhydryl contents:

The disulfide bond content was calculated using Eq. (2):

$$SS\ content\ (\mu mol/g\ protein) = \frac{Total\ SH - free\ SH}{2} \quad (2)$$

Free sulfhydryl content represents the reactive thiol groups accessible under non-denaturing assay conditions, whereas total sulfhydryl content represents thiol groups detected under denaturing conditions in the presence of SDS and urea. Therefore, the calculated disulfide bond content was used as an indirect estimate of disulfide-associated bonding in the heat-treated fermented chickpea powders.

2.3.5. Protein solubility and surface hydrophobicity (H_0)

Sample solutions (100 mg/mL) were prepared as described in Section 2.3.2. The protein concentration in the supernatant was determined by using a BCA assay, with bovine serum albumin used as the standard. 125 μL of sample was mixed with 1 mL BCA reagent, followed by incubating at 37 °C for 30 min. The absorbance at 562 nm was measured using a UV–Vis spectrometer. Protein solubility was calculated using following equation (Eq. (3)):

$$Protein\ solubility\ (\%) = \frac{C_{sup}}{C_{total} \times Crude\ protein\ content} \times 100 \quad (3)$$

where C_{sup} is the protein concentration in the supernatant C_{total} is the initial concentration of chickpea powder in the dispersion.

The H_0 value was determined using ANS as a fluorescence probe according to the method [19] with slight modifications. Sample solutions (100 mg/mL) were prepared as described in Section 2.3.2. Supernatant was diluted with DW to obtain concentrations of 1, 2, 4, 8, and 10 mg/mL. 2 mL of each diluted sample was mixed with 20 μL of 8 mM ANS solution and incubated in the dark for 30 min. Fluorescence intensity was measured using a fluorophotometer (FluoroMax-4, Horiba Jobin Yvon, Edison, NJ, USA) with an excitation wavelength of 380 nm and an emission wavelength range of 400–600 nm. The H_0 value was calculated as the initial slope of the linear regression between fluorescence intensity and protein concentration.

2.4. Preparation of artificial fat (AF)

Coconut oil-based artificial fat (AF) systems were prepared using a modified hot emulsification method [20]. Heat-treated fermented chickpea powders obtained at 0, 24, 48, and 72 h of fermentation were dispersed in distilled water at 10% (*w/w*), and the pH of each dispersion was adjusted to 12.0 using 4 M NaOH to obtain alkaline-extracted soluble chickpea fractions. The dispersions were stirred at 25 °C and 150 rpm for 1 h and then centrifuged at 2000 ×*g* for 10 min at 20 °C. The supernatant was collected and neutralized to pH 7.0 using 1 M HCl before use.

For each AF formulation, melted coconut oil, neutralized 10% fermented chickpea extract, and NaCl were mixed at 100 g, 13 g, and 0.5 g, respectively, corresponding to 88.1%, 11.5%, and 0.4% of the final formulation (Table S1). The same formulation was used for all AF systems, with the groups differing only in the fermentation time of the

chickpea powder used to prepare the neutralized alkaline-extracted fraction. The fermented chickpea extract and NaCl were preheated at 45 °C for 5 min, and coconut oil was separately melted at 45 °C for 15 min. The melted coconut oil was gradually added to the aqueous chickpea extract phase while homogenizing at 14,000 rpm for 3 min. The resulting emulsified AF systems were kept at room temperature for 30 min, transferred into 50 mL conical tubes, stored at 4 °C overnight, and equilibrated at 20 °C before characterization. The resulting samples were labeled AF-0 h, AF-24 h, AF-48 h, and AF-72 h.

Alkaline extraction at pH 12 was used to obtain soluble chickpea fractions for AF preparation. Because strong alkaline conditions can induce protein unfolding, dissociation, or structural rearrangement, the AF results were interpreted as the functional behavior of neutralized alkaline-extracted chickpea fractions obtained from heat-treated fermented powders, rather than as the direct behavior of native proteins immediately after fermentation.

2.5. Characterization of artificial fat

2.5.1. Visual appearance and optical microscopy

The visual appearance of beef tallow, coconut oil, and AFs was photographed using a studio photo box (Shenzhen Puluz Technology, Guangdong, China) equipped with dual-direction LED lighting (1690 lm). The microstructures of beef tallow, coconut oil, and AFs were observed using an optical microscope (Leica ICC50 HD, Leica Microsystems, Heerbrugg, Switzerland). Images were taken at 400× magnification.

2.5.2. Zeta potential

Each AF was diluted 100 times with DW, and the zeta potential was measured using a Zetasizer Nano ZS analyzer (Malvern Panalytical, Malvern, UK). The diluted samples were equilibrated at 25 °C for 120 s, and each sample was measured in triplicate. The average value was used for data analysis.

2.5.3. Emulsion properties

The emulsion activity index (EAI), emulsion stability index (ESI), heat-treated emulsion activity index (HEAI), and thermal stability index (TSI) of the coconut oil-based artificial fat (AF) systems were determined according to a previously reported method with slight modifications [21]. Briefly, 25 μL of each AF sample was collected and immediately diluted with 5 mL of 0.5% SDS solution. The diluted sample was vortexed, and the absorbance was measured at 500 nm. For ESI determination, the absorbance was measured immediately after dilution (A_0) and after 10 min of standing (A_{10}). For HEAI determination, the AF samples were heated at 95 °C for 30 min and cooled in cold water for 10 min before dilution and absorbance measurement. TSI was subsequently calculated from the EAI and HEAI values to represent the retention of apparent emulsion activity after heat treatment.

EAI, ESI, HEAI, and TSI were calculated using the following equations (Eqs. (4), (5), (6), and (7)):

$$EAI\ (m^2/g) = \frac{2 \times 2.303 \times A_0 \times N}{c \times \varphi \times 10^4} \tag{4}$$

$$\mathrm{E}SI\ (min) = \frac{A_0}{A_0 - A_{10}} \times \Delta \mathrm{t} \tag{5}$$

$$HEAI\ (m^2/g) = \frac{2 \times 2.303 \times AH \times N}{c \times \varphi \times 10^4} \tag{6}$$

$$TSI\ (\%) = \frac{HEAI}{EAI} \times 100 \tag{7}$$

where A_0 is the absorbance measured immediately after dilution, A_{10} is the absorbance measured after 10 min, AH is the absorbance of the heat-treated sample, N is the dilution factor, C is the estimated protein concentration in each AF system, φ is the oil volume fraction, and Δt is the standing time of 10 min. The value of C was estimated from the amount of chickpea-derived extract incorporated into the AF formulation and the sample-specific crude protein content of the corresponding fermented chickpea powder. The protein concentration was therefore used as an estimated normalization factor for EAI and HEAI calculations, rather than as a directly measured soluble protein concentration in the neutralized alkaline extract.

2.5.4. Rheological properties

The rheological properties of the AF systems were measured using a rotational rheometer equipped with a 20 mm parallel plate geometry and a gap of 1000 μm. Before measurement, each sample was placed between the plates and equilibrated for 2 min. All rheological measurements were performed at 20 °C with a soak time of 120 s.

Apparent viscosity was measured by flow sweep analysis over a shear rate range of 0.01–100 s^{-1}. The flow behavior was fitted to the Ostwald–de Waele power-law model using the following equation (Eq. (8)):

$$\eta = K \bullet \dot{\gamma}^{\dot{m}} \tag{8}$$

where η is the apparent viscosity, K is the consistency coefficient, $\dot{\gamma}$ is the shear rate, and m is the power-law exponent. Negative m values indicate a decrease in apparent viscosity with increasing shear rate, corresponding to shear-thinning behavior.

An amplitude sweep was first performed over a strain range of 0.01–100% at an angular frequency of 10 rad/s to determine the linear viscoelastic region (LVR). A strain of 0.1%, which was within the LVR for all samples, was subsequently selected for frequency sweep measurements. Frequency sweeps were conducted over an angular frequency range of 0.1–100 rad/s, and the storage modulus (G') and loss modulus (G'') were recorded as a function of angular frequency.

2.5.5. X-ray diffraction (XRD)

The crystalline properties of beef tallow, coconut oil, and AFs were characterized using an XRD (EMPYREAN, Panalytical, Netherlands) operated at 40 kV and 30 mA. The diffraction patterns were scanned to obtain 2θ angles between 5° and 40° at 3.5°/min.

2.5.6. Differential scanning calorimetry (DSC)

The melting and crystallization behaviors of beef tallow, coconut oil, and AFs were analyzed using a differential scanning calorimeter (DSC; Q2000, TA Instruments, New Castle, DE, USA). 8 mg of each sample was weighed into an aluminum pan and hermetically sealed. The samples were first heated to 90 °C and held for 30 min to eliminate crystalline history. Subsequently, the samples were cooled to −40 °C at rate of 5 °C/min and maintained for 10 min. Finally, the samples were reheated to 100 °C at heating rate of 5 °C/min, and the melting thermograms were recorded.

2.6. Statistical analysis

Statistical analyses were performed using SPSS software (Version 26, SPSS, IL, USA). All experiments were conducted at least in triplicate, and the results are presented as the mean ± standard deviation. One-way analysis of variance (ANOVA) and Duncan's multiple range test were used to evaluate significant differences among the groups. Differences were considered statistically significant at $p < 0.05$. Pearson's correlation analysis was performed using SPSS software, reporting significance levels of $^{*}p < 0.05$, $^{**}p < 0.01$, $^{***}p < 0.001$, and $^{****}p < 0.0001$ for significant correlations. Pearson correlation analysis was performed using replicate-level paired data obtained from four fermentation times with three independent biological replicates per condition ($n = 12$). For each replicate, the structural and functional properties of the chickpea fractions and the corresponding emulsion properties of the AF systems

were obtained from the same independently prepared fermentation batch, thereby preserving replicate-level pairing between the datasets. The analysis was used as an exploratory assessment of structure–function associations, and the resulting correlations were not interpreted as direct evidence of causality.

3. Results and discussion

3.1. Fermentation-associated structural reorganization and functional changes in chickpea proteins

3.1.1. Changes in protein molecular profile and aggregation behavior

SDS-PAGE was used to examine changes in the molecular weight distribution of chickpea proteins across fermentation times (Fig. 1A). The unfermented chickpea powder exhibited distinct protein bands corresponding to the major chickpea storage proteins, including vicilin minor subunits (approximately 25–28 kDa), vicilin (48–50 kDa), and convicilin (68–72 kDa) [16]. After 24 h of fermentation, the intensity of the high-molecular-weight protein bands, particularly those above 60 kDa, became markedly weaker. Prolonged fermentation further reduced the overall band intensity, indicating progressive changes in the molecular profile of chickpea storage proteins. This pattern is consistent with fermentation-associated proteolytic modification and redistribution of storage protein fractions rather than a reduction in crude protein content itself. Indeed, the crude protein content increased from 23.10% in the unfermented chickpea powder to 34.58% after 72 h of fermentation (Table 1). Rhizopus spp. can secrete proteolytic enzymes during SSF, which may contribute to the hydrolysis of legume storage proteins into lower-molecular-weight peptides and soluble nitrogenous compounds. Accordingly, the SDS-PAGE patterns suggest that increasing fermentation time was associated with changes in the molecular weight distribution and subunit profile of chickpea proteins, consistent with partial hydrolysis and subsequent structural reorganization. Similar changes in protein profiles have been reported in fermented chickpea and other legume matrices [11,14].

Turbidity analysis further indicated fermentation-associated changes in the dispersion and aggregation behavior of chickpea proteins (Fig. 1B). Turbidity initially decreased after fermentation, suggesting a shift toward more readily dispersed protein fractions or a reduction in the abundance of larger aggregates [22]. This pattern is consistent with partial proteolytic modification during the early stage of fermentation. In contrast, prolonged fermentation resulted in increased turbidity, suggesting greater aggregation or reduced dispersibility of the protein fractions. Such behavior may be associated with reassociation among structurally modified protein molecules through hydrophobic interactions, hydrogen bonding, or disulfide-associated interactions [23]. Thus, fermentation did not produce a continuous improvement in protein dispersibility; rather, moderate fermentation was associated with improved dispersion, whereas prolonged fermentation favored a less dispersible protein state.

Overall, the SDS-PAGE and turbidity results indicate time-dependent changes in the molecular distribution and aggregation state of chickpea proteins across fermentation conditions. These observations provide a structural basis for examining the accompanying changes in secondary structure, intermolecular interactions, and functional properties.

3.1.2. Secondary structural reorganization

The secondary structure of the soluble protein fraction from heat-treated fermented chickpea powders was estimated by circular dichroism (CD) spectroscopy (Table 2). The unfermented sample contained 4.75% α-helix, 27.95% β-sheet, 15.75% β-turn, and 51.55% random coil. With increasing fermentation time, the α-helix content progressively decreased from 4.75% to 1.70% after 72 h, whereas the β-sheet content increased from 27.95% to 34.25%. The β-turn content decreased slightly at 24 h but subsequently increased, reaching 20.95% at 72 h, while the random coil fraction gradually decreased from 51.55% to 43.10%. This observation is consistent with the SDS-PAGE results, which demonstrated progressive degradation of the major chickpea storage proteins.

The reduction in α-helix content indicates a lower proportion of helical organization in the soluble protein fraction after fermentation. This pattern is consistent with the changes observed by SDS-PAGE and may reflect fermentation-associated proteolytic modification and conformational rearrangement of chickpea proteins. Proteolysis and other biochemical reactions occurring during Rhizopus fermentation can alter peptide-chain organization and intramolecular interactions, thereby contributing to changes in secondary structural organization. Similar reductions in α-helical content have been reported for plant proteins subjected to enzymatic hydrolysis or fermentation-related modification [24,25].

The concurrent increase in β-sheet content suggests an enrichment of β-structured components within the soluble protein fraction during prolonged fermentation. Because β-sheet structures are stabilized by inter- and intramolecular hydrogen bonding, this change may reflect increased molecular association following conformational rearrangement. When considered together with the increase in turbidity during prolonged fermentation, the CD results are consistent with a shift toward a more associated and less readily dispersed protein state. The increase in β-turn content after 48 h further supports progressive conformational reorganization rather than simple unfolding of the original protein structure.

Collectively, the CD results indicate fermentation-associated reorganization of the secondary structure of soluble chickpea proteins,

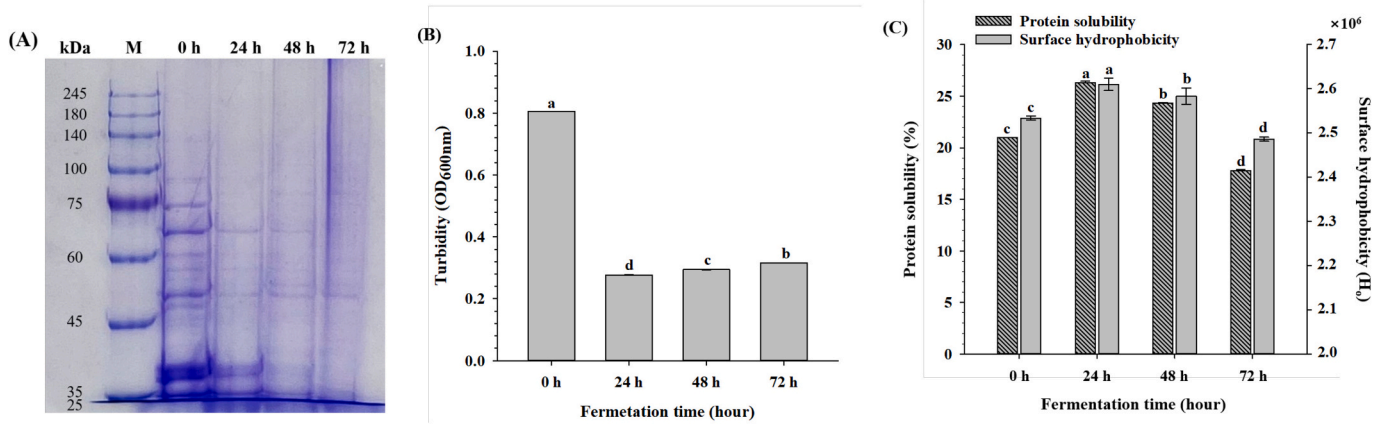


Fig. 1. SDS-PAGE profiles (A), turbidity (B), and protein solubility and surface hydrophobicity (C) of chickpea powders with different fermentation times. M: protein molecular weight marker.

Table 2
Content of secondary structures in chickpea powders with different fermentation times.

Fermentation time (hour)	α-Helix (%)	β-Sheet (%)	β-Turn (%)	Random coil (%)
0	4.75 ± 0.15^{a}	27.95 ± 0.15^{c}	15.75 ± 0.55^{c}	51.55 ± 0.25^{a}
24	3.95 ± 0.25^{b}	31.75 ± 0.35^{b}	14.50 ± 0.10^{bc}	49.80 ± 0.50^{a}
48	2.50 ± 0.00^{c}	33.87 ± 1.65^{ab}	16.70 ± 1.59^{b}	46.93 ± 0.57^{b}
72	1.70 ± 0.10^{d}	34.25 ± 1.75^{a}	20.95 ± 0.05^{a}	43.10 ± 1.70^{c}

Values are presented as the mean ± SD ($n = 3$). Different letters within the same column indicate significant differences ($p < 0.05$).

characterized by a progressive decrease in α-helical components and an increase in β-structured components. Because the CD analysis was performed on soluble fractions obtained from heat-treated fermented chickpea powders rather than purified protein isolates, these results are interpreted as relative structural differences among the fractions under the present preparation conditions.

3.1.3. Alterations in sulfhydryl groups and disulfide bonding

The contents of total –SH, free –SH, and calculated S—S were determined to evaluate fermentation-associated changes in the thiol–disulfide state of chickpea proteins (Table 3). The total –SH content continuously decreased from 357.36 μmol/g in the unfermented sample to 170.00 μmol/g after 72 h of fermentation. Free –SH content also decreased markedly from 214.91 μmol/g to 94.12 μmol/g after 24 h and further to 60.47 μmol/g after 48 h, followed by a slight increase at 72 h. In contrast, the calculated S—S content increased from 71.22 μmol/g in the unfermented sample to 97.04 and 98.63 μmol/g after 24 and 48 h, respectively, before decreasing to 49.63 μmol/g at 72 h.

The reduction in total and free –SH indicates changes in the availability of thiol groups across fermentation conditions. Free –SH groups are commonly used as indicators of changes in protein conformation and the accessibility or consumption of reactive thiol residues [26,27]. The marked reduction in free –SH during the early and intermediate stages of fermentation is consistent with the consumption or reduced accessibility of thiol groups through processes such as oxidation, thiol–disulfide exchange, or structural rearrangement. The concomitant increase in calculated S—S content at 24–48 h is therefore consistent with greater disulfide-associated bonding under these conditions [28]. However, because S—S content was estimated indirectly from total and free sulfhydryl contents, these values do not distinguish between intra- and intermolecular disulfide linkages [29].

The decline in calculated S—S content after 72 h suggests a reduction in disulfide-associated bonding under prolonged fermentation conditions. This change may reflect the combined effects of extended proteolytic modification and structural rearrangement of the protein fractions. Accordingly, rather than indicating direct disruption of a defined cross-linked network, the 72 h condition appears to represent a protein state with a less favorable thiol–disulfide balance than that observed after 24–48 h of fermentation.

Together with the SDS-PAGE, turbidity, and CD results, these findings indicate that fermentation time was associated with non-linear changes in the thiol–disulfide state of chickpea proteins. Moderate fermentation was associated with greater disulfide-related reorganization, whereas prolonged fermentation resulted in lower calculated disulfide-associated bonding. These differences may contribute to changes in protein flexibility, association, and subsequent functional behavior in the AF systems.

Table 3
Sulfhydryl group and disulfide bond of chickpea powders with different fermentation times.

Fermentation time (hour)	Total –SH (μmol/g)	Free –SH (μmol/g)	S–S (μmol/g)
0	357.36 ± 0.64^{a}	214.91 ± 0.18^{a}	71.22 ± 0.40^{c}
24	288.21 ± 0.45^{b}	94.12 ± 0.15^{b}	97.04 ± 0.15^{b}
48	257.74 ± 0.54^{c}	60.47 ± 0.07^{d}	98.63 ± 0.29^{a}
72	170.00 ± 0.11^{d}	70.74 ± 0.06^{c}	49.63 ± 0.03^{d}

Values are presented as the mean ± SD ($n = 3$). Different letters within the same column indicate significant differences ($p < 0.05$).

3.1.4. Exposure of hydrophilic and hydrophobic moieties

Protein solubility and surface hydrophobicity (H_o) were evaluated to determine whether fermentation-associated structural reorganization was accompanied by changes in the functional properties of chickpea proteins (Fig. 1C). Protein solubility was significantly affected by fermentation time, increasing from approximately 21% in the unfermented sample to the highest value after 24 h of fermentation. The 48 h sample maintained a higher solubility than the unfermented sample, although the value was slightly lower than that of the 24 h sample. In contrast, the 72 h sample exhibited the lowest solubility, reaching 17.79% ($p < 0.05$). These results indicate that moderate fermentation was associated with improved protein dispersibility, whereas prolonged fermentation reduced the proportion of soluble protein.

The increased solubility after 24–48 h may be related to partial proteolytic modification, which can reduce protein molecular size and increase the accessibility of hydrophilic groups, thereby enhancing protein–water interactions [30]. This interpretation is consistent with the SDS-PAGE and turbidity results, which indicated changes in protein molecular profiles and improved dispersibility during the early and intermediate fermentation stages. Conversely, the marked decrease in solubility at 72 h may reflect increased association or aggregation of structurally modified protein fractions. Similar decreases in protein solubility have been reported following extensive structural modification of globular proteins [22].

H_o exhibited a similar fermentation-dependent pattern, with the highest value observed at 24 h, followed by the 48 h, 0 h, and 72 h samples (Fig. 1C). The increase in H_o after moderate fermentation is consistent with greater accessibility of hydrophobic regions resulting from partial conformational rearrangement or proteolytic modification. Increased accessibility of hydrophobic domains is generally favorable for the interfacial activity of protein-based emulsifiers because it can promote interactions with the lipid phase [31]. In contrast, the lower H_o observed at 72 h may reflect reduced accessibility of hydrophobic regions as a result of extensive structural modification or aggregation [11].

Overall, the solubility and H_o results indicate that fermentation time altered the balance between protein dispersibility and hydrophobic-domain accessibility. Among the tested conditions, 24 h fermentation provided the most favorable combination of solubility and surface hydrophobicity, whereas prolonged fermentation for 72 h reduced both properties. When considered together with the molecular, secondary structural, and thiol–disulfide results, these findings support a fermentation-associated restructuring of chickpea proteins that was subsequently related to differences in their performance within the coconut oil-based AF systems.

3.2. Emulsion and interfacial performance of artificial fat systems

3.2.1. Microstructure and electrostatic stability

The microstructure and electrostatic stability of the AF systems were evaluated to examine whether fermentation-associated differences in chickpea protein fractions were accompanied by changes in the

organization of the dispersed lipid phase (Figs. 2 and 3). Visual observation revealed clear differences among beef tallow, coconut oil, and the AF systems prepared with chickpea-derived emulsifying fractions (Fig. 2A). Beef tallow and coconut oil formed transparent liquid phases upon heating at 45 °C and returned to solid-like states after cooling. In contrast, all AF systems exhibited an opaque appearance after emulsification and cooling, consistent with the formation of dispersed lipid systems rather than simple crystalline fat phases.

Optical microscopy further revealed differences in the internal organization of the samples after cooling (Fig. 2B). Beef tallow exhibited a dense crystalline network composed of needle-like crystals [32,33], whereas coconut oil showed a characteristic spherulitic morphology with radially arranged needle-like crystals, consistent with previous observations for native coconut oil [34]. In contrast, the AF systems exhibited droplet-based microstructures, indicating that emulsification with chickpea-derived fractions produced dispersed coconut oil phases. Among the AF systems, AF-24 h and AF-48 h showed visually smaller and more uniformly distributed droplets than AF-0 h, whereas AF-72 h exhibited a broader and less homogeneous droplet distribution. These observations suggest that moderate fermentation was associated with a more homogeneous dispersed structure, while prolonged fermentation was less favorable for maintaining droplet uniformity.

The zeta potential results were consistent with these microstructural differences (Fig. 3). All AF systems showed negative zeta potential values, indicating the presence of negatively charged components at the droplet surface. AF-0 h exhibited a zeta potential of −42.23 mV, while the absolute zeta potential increased after moderate fermentation and reached its highest value in AF-24 h. In contrast, AF-72 h showed the lowest absolute zeta potential among the AF systems (−39.73 mV). A larger absolute zeta potential is generally associated with greater electrostatic repulsion between dispersed droplets and may reduce their tendency to aggregate [35]. Accordingly, the greater absolute zeta potential of AF-24 h was consistent with its more homogeneous droplet distribution.

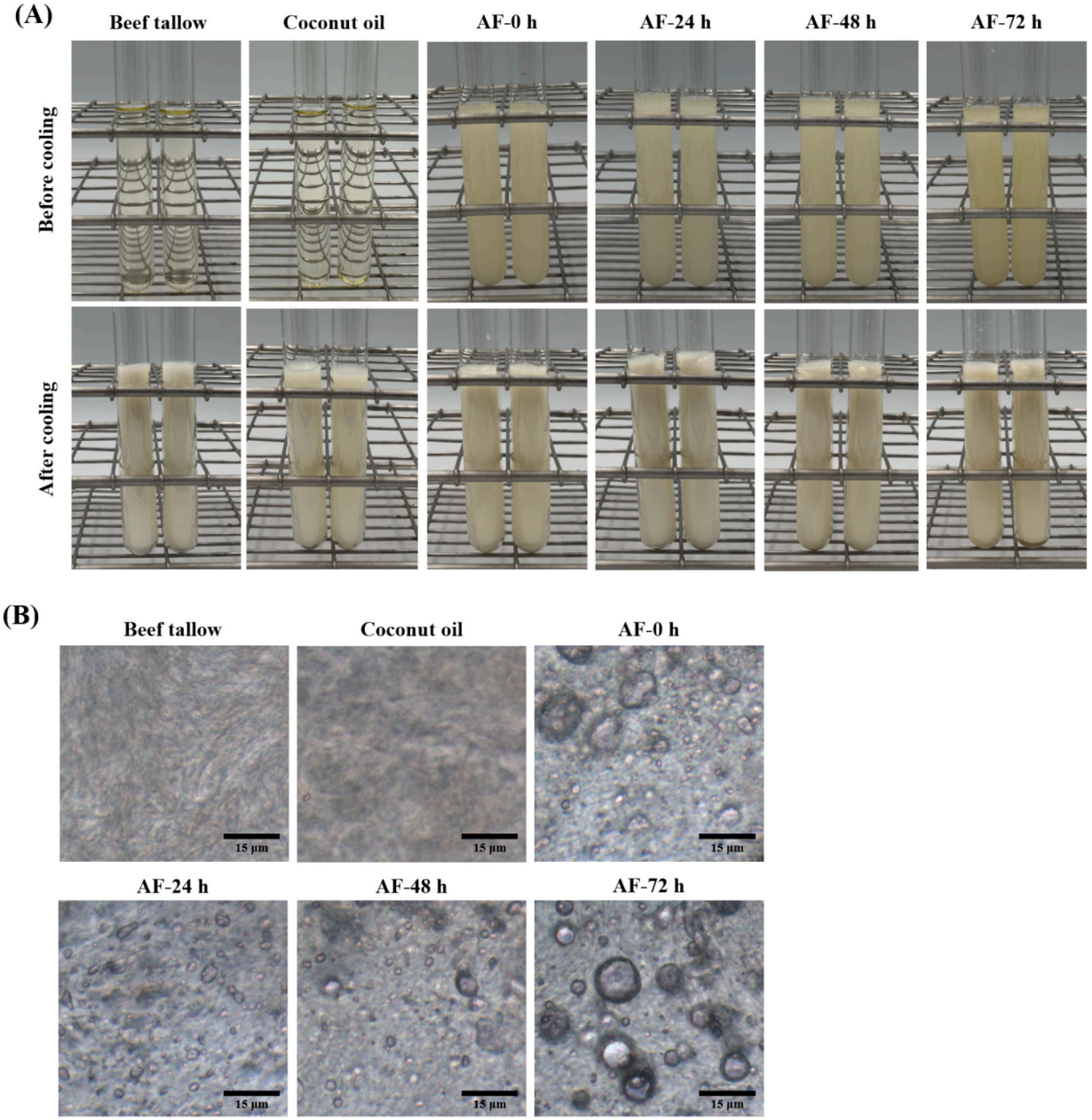


Fig. 2. Visual appearance (A) and optical microscopy image (15 μm scale bar) (B) of beef tallow, coconut oil, and artificial fats (AFs) using chickpea powders with different fermentation times.

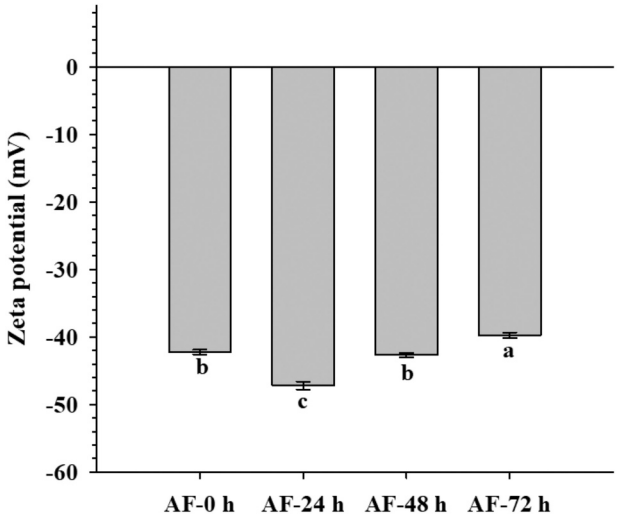


Fig. 3. Zeta potential of artificial fats (AFs) using chickpea powders with different fermentation times.

The microstructural and zeta potential patterns were also consistent with the solubility and surface hydrophobicity trends of the corresponding chickpea fractions. The 24 h fermented fraction exhibited the most favorable balance between protein dispersibility and hydrophobic-domain accessibility, which may have contributed to improved interactions with the oil–water interface[36,37]. In contrast, AF-72 h showed both a less homogeneous droplet structure and a lower absolute zeta potential, consistent with the reduced solubility and H_o of the corresponding chickpea fraction. Overall, these findings indicate that fermentation-associated differences in chickpea protein fractions were accompanied by measurable changes in droplet organization and electrostatic stabilization of the AF systems.

3.2.2. *Emulsion activity, stability and thermal resistance*

The emulsion activity index (EAI), emulsion stability index (ESI), heat-treated emulsion activity index (HEAI), and thermal stability index (TSI) were determined to evaluate the emulsion performance of coconut oil-based AF systems prepared with alkaline-extracted chickpea fractions obtained at different fermentation times (Fig. 4). After recalculation using the sample-specific crude protein content of each fermented chickpea powder, AF-24 h showed the highest EAI value of 7.75 m^2/g, followed by AF-48 h, AF-0 h, and AF-72 h. This result indicates that the 24 h fermented chickpea fraction provided the most favorable condition for apparent droplet formation among the tested AF systems. Previous studies have similarly reported improved emulsifying activity of chickpea-based materials following solid-state fermentation [30].

The higher EAI of AF-24 h was associated with the higher solubility and H_o of the corresponding chickpea fraction. Greater protein dispersibility and accessibility of hydrophobic regions can favor diffusion and association of protein molecules with the oil–water interface in protein-stabilized emulsions [36,38]. Partial proteolytic modification during moderate fermentation may also increase molecular flexibility and exposure of both hydrophilic and hydrophobic regions, thereby supporting emulsifying performance [30,36]. In contrast, the markedly lower EAI of AF-72 h was consistent with its lower protein solubility, reduced H_o, and less homogeneous droplet distribution. These observations suggest that prolonged fermentation was less favorable for maintaining the functional characteristics required for effective droplet formation.

The ESI values showed a different trend. AF-48 h and AF-24 h exhibited the highest ESI values, at 101.72 and 101.00 min, respectively, followed by AF-72 h and AF-0 h. These results indicate that the moderately fermented fractions were associated with greater short-term retention of the dispersed AF structure under the present measurement conditions. This behavior may reflect differences in protein conformation, dispersibility, and interfacial association among the chickpea fractions [36]. However, because ESI was calculated from absorbance retention after dilution over a short standing period, it should be interpreted as an operational index of short-term emulsion retention rather than a direct measurement of interfacial film strength.

Thermal retention was further evaluated using HEAI and TSI. AF-24 h showed the highest HEAI value of 8.36 m^2/g, followed by AF-48 h, AF-0 h, and AF-72 h. TSI was also highest in AF-24 h, followed by AF-48 h, AF-72 h, and AF-0 h. These results indicate that the 24 h fermented chickpea fraction was most favorable for maintaining apparent emulsion activity after heat treatment. The higher HEAI and TSI values of AF-24 h were associated with its higher protein solubility, greater H_o, and greater calculated S—S content. These structural and functional characteristics may have contributed to the ability of the dispersed system to retain apparent emulsion activity after heating.

Notably, TSI values for AF-24 h and AF-48 h exceeded 100%. This does not necessarily indicate that heat treatment improved the intrinsic mechanical stability of the emulsion interface. Rather, heat treatment may have altered droplet structure, protein association, or light-scattering behavior, thereby increasing the measured absorbance. Therefore, TSI was interpreted as an operational thermal-retention index of apparent emulsion activity under the present assay conditions. Similar caution is required for other absorbance-based emulsion indices, which reflect changes in turbidity or light scattering rather than direct interfacial mechanical properties.

Overall, the corrected emulsion indices indicate that moderate fermentation, particularly for 24 h, was associated with more favorable droplet formation and thermal retention in the coconut oil-based AF systems. The 48 h fermented fraction showed comparable short-term emulsion retention but lower EAI and HEAI than AF-24 h, whereas prolonged fermentation for 72 h resulted in lower apparent emulsion activity. These findings support an association between the functional state of the alkaline-extracted chickpea fractions and the emulsion performance of the AF systems. However, direct interfacial rheology, interfacial tension, and interfacial protein characterization were not performed; therefore, the underlying interfacial mechanisms cannot be established from the present data alone. In addition, the protein concentration used for the emulsion indices was estimated from the crude protein content of the corresponding chickpea powders rather than directly quantified in the neutralized alkaline extracts; therefore, possible differences in protein extraction efficiency among fermentation treatments were not fully accounted for.

3.2.3. *Structure-functional correlations between protein attributes and emulsion properties*

Pearson correlation analysis was performed to explore the relationships between the structural and functional attributes of the heat-treated fermented chickpea samples and the emulsion indices of the corresponding coconut oil-based AF systems (Table 4). Because the AF systems were prepared using neutralized alkaline-extracted fractions obtained from heat-treated fermented chickpea powders, the correlations were interpreted as structure–function associations under the present preparation conditions rather than as direct evidence of causality. In protein-stabilized emulsions, emulsion behavior can be influenced by multiple sequential processes, including protein diffusion, adsorption, conformational rearrangement, and association at the oil–water interface [6,38,39]. Accordingly, the observed relationships were interpreted in relation to the combined structural and functional state of the chickpea fractions rather than fermentation time alone.

EAI showed strong positive correlations with calculated S—S content ($r = 0.935$, $p < 0.0001$), protein solubility ($r = 0.992$, $p < 0.0001$), and H_o ($r = 0.968$, $p < 0.0001$), and was negatively correlated with β-turn content ($r = -0.806$, $p < 0.01$). These relationships indicate that apparent droplet formation was closely associated with protein

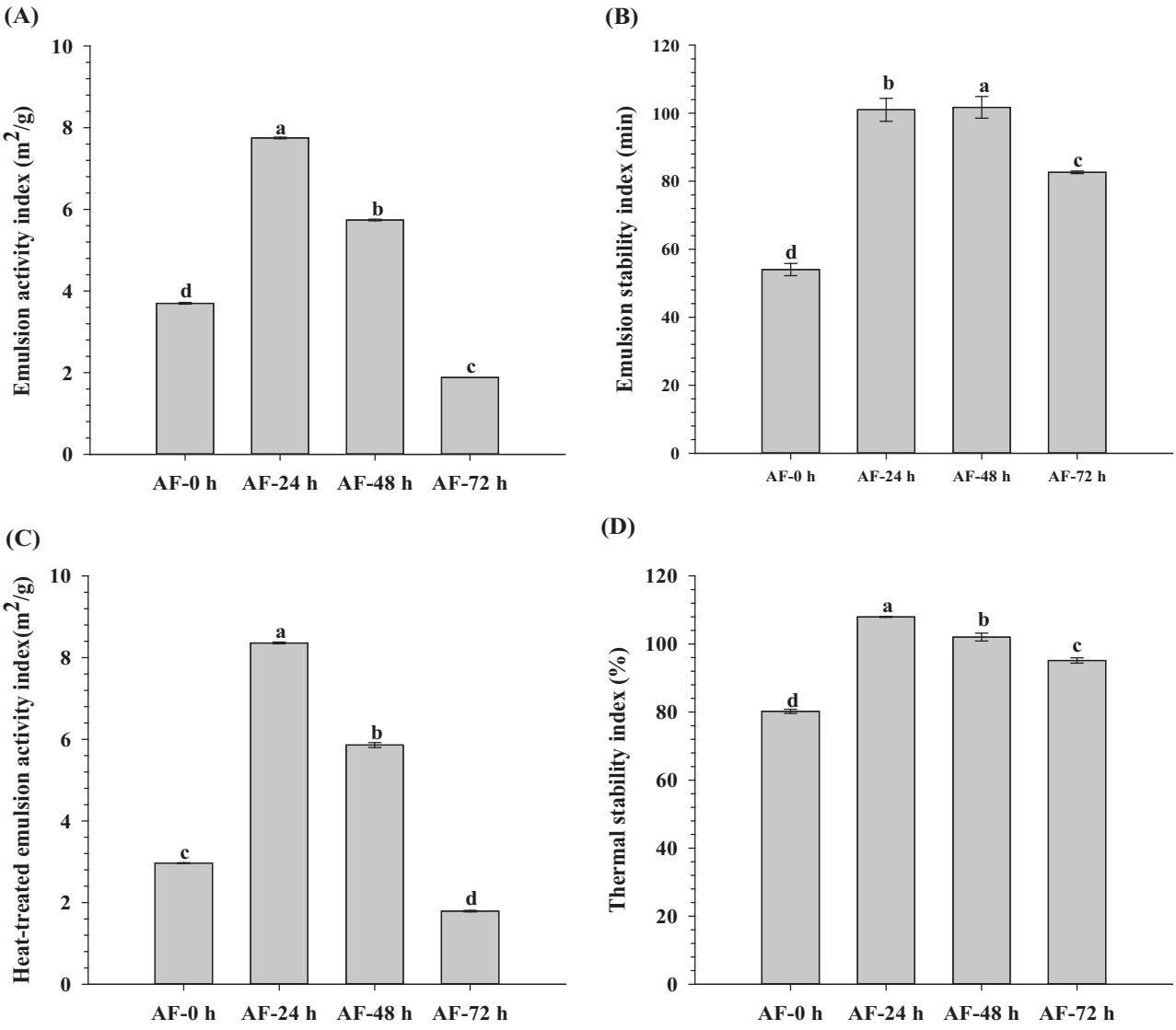


Fig. 4. Emulsion performance of coconut oil-based artificial fat (AF) systems prepared with alkaline-extracted chickpea fractions obtained at different fermentation times. (A) Emulsion activity index (EAI), (B) emulsion stability index (ESI), (C) heat-treated emulsion activity index (HEAI), and (D) thermal stability index (TSI). Different letters indicate significant differences among samples ($p < 0.05$).

Table 4
Exploratory Pearson correlations between structural and functional attributes of heat-treated fermented chickpea samples and emulsion indices of the corresponding artificial fat systems.

Emulsion index	α-Helix	β-Sheet	β-Turn	Random coil	Total –SH	Free –SH	S–S	Protein solubility	H_o
EAI	0.401	−0.046	−0.806**	0.509	0.402	−0.173	0.935****	0.992****	0.968****
ESI	−0.473	0.689*	−0.063	−0.343	−0.455	−0.881***	0.589*	0.589*	0.587*
HEAI	0.294	0.062	−0.730**	0.401	0.280	−0.289	0.907****	0.974****	0.951****
TSI	−0.370	0.624*	−0.142	−0.267	−0.412	−0.824***	0.574	0.627*	0.616*

Pearson correlation coefficients (r) were calculated using replicate-level paired data obtained from four fermentation times (0, 24, 48, and 72 h), with three independent biological replicates per condition ($n = 12$). Structural and functional attributes and the corresponding AF emulsion properties were obtained from the same independently prepared fermentation batches. S—S represents the calculated disulfide-associated bonding estimated from total and free sulfhydryl contents. TSI represents the thermal retention of apparent emulsion activity calculated from HEAI relative to EAI. Correlations were interpreted as exploratory structure–function associations rather than evidence of causality. Asterisks indicate significance levels: $p < 0.05$, $p < 0.01$, $p < 0.001$, and $p < 0.0001$.

dispersibility, hydrophobic-domain accessibility, and the thiol–disulfide state of the chickpea fractions. Greater protein solubility can facilitate diffusion toward the oil–water interface, whereas greater accessibility of hydrophobic regions can favor association with the lipid phase [36,37]. The positive association with calculated S—S content further suggests that disulfide-associated reorganization may have contributed to the functional state of the protein fractions. Accordingly, the high EAI of AF-24 h coincided with a favorable combination of solubility, H_o, and calculated S—S content.

HEAI exhibited a similar correlation pattern to EAI, showing positive correlations with calculated S—S content ($r = 0.907$, $p < 0.0001$), protein solubility ($r = 0.974$, $p < 0.0001$), and H_o ($r = 0.951$, $p < 0.0001$),

and a negative correlation with β-turn content ($r = -0.730$, $p < 0.01$). These associations indicate that apparent emulsion activity after heat treatment was related to the same protein characteristics associated with initial emulsion activity. However, because HEAI was determined using an absorbance-based assay, it should be interpreted as heat-treated apparent emulsion activity rather than as direct evidence of strengthened interfacial films.

ESI showed a distinct correlation pattern. It was positively correlated with β-sheet content ($r = 0.689$, $p < 0.05$), calculated S—S content ($r = 0.589$, $p < 0.05$), protein solubility ($r = 0.589$, $p < 0.05$), and H_o ($r = 0.587$, $p < 0.05$), and negatively correlated with free –SH content ($r = -0.881$, $p < 0.001$). These results indicate that short-term emulsion retention was associated with the combined conformational and functional state of the chickpea fractions rather than with a single structural variable. The positive association between β-sheet content and ESI should be interpreted cautiously because β-structured organization may contribute differently depending on the extent of protein association or aggregation. Indeed, prolonged fermentation was accompanied by greater β-sheet content but lower solubility and less favorable emulsion performance, indicating that increased β-structured organization alone was not sufficient to explain emulsion behavior.

TSI was positively correlated with β-sheet content ($r = 0.624$, $p < 0.05$), protein solubility ($r = 0.627$, $p < 0.05$), and H_o ($r = 0.616$, $p < 0.05$), and negatively correlated with free –SH content ($r = -0.824$, $p < 0.001$). These associations suggest that thermal retention of apparent emulsion activity was related to both protein dispersibility and fermentation-associated conformational differences. However, because TSI was calculated as the ratio of HEAI to EAI, it should be interpreted as an operational thermal-retention index rather than as an independent measurement of thermal or interfacial stability.

Overall, the exploratory correlation analysis indicates that EAI and HEAI were most strongly associated with protein solubility, H_o, and calculated S—S content, whereas ESI and TSI were additionally associated with β-sheet and free –SH contents. These findings support the presence of structure–function associations between the fermentation-modified chickpea fractions and the emulsion performance of coconut oil-based AF systems. Nevertheless, because the analysis was correlation-based and direct interfacial measurements were not performed, these relationships should not be interpreted as mechanistic proof that protein restructuring alone determined AF formation or stability.

3.3. Rheological behavior and stabilization of artificial fat systems

3.3.1. Shear-thinning behavior and viscosity characteristics

The apparent viscosity of the AF systems was evaluated to determine whether fermentation-associated differences in the chickpea fractions were reflected in the bulk rheological behavior of the resulting emulsified systems (Fig. 5A and Table 5). All AF samples exhibited a progressive decrease in apparent viscosity with increasing shear rate, demonstrating shear-thinning behavior. Such behavior is commonly observed in structured emulsion systems and can arise from deformation and alignment of dispersed components, disruption of weakly associated structures, and rearrangement of interactions under flow [40].

Differences among the AF systems were most pronounced at low shear rates, where interactions among dispersed components contribute more strongly to bulk viscosity. AF-24 h exhibited the highest apparent viscosity, followed by AF-48 h, AF-0 h, and AF-72 h. This pattern was consistent with the microstructural and emulsion-related observations, particularly the relatively homogeneous droplet distribution and greater absolute zeta potential observed for AF-24 h. The higher apparent viscosity of AF-24 h indicates greater resistance to flow and is consistent with a more developed internal structure within the AF system. The corresponding chickpea fraction also showed relatively high protein solubility, H_o, and calculated S—S content, suggesting that its structural and functional state may have contributed to the observed bulk rheological behavior. Previous studies have similarly shown that the organization of dispersed components can influence the rheological properties of emulsion systems [41].

In contrast, AF-72 h exhibited the lowest apparent viscosity. This behavior coincided with lower protein solubility, H_o, and calculated S—S content, as well as a less homogeneous droplet distribution and less

Table 5
Power-law parameters of artificial fat (AF) systems prepared with chickpea fractions obtained at different fermentation times.

Samples	R^2	Power-law exponent, m	Consistency coefficient, K ($Pa \cdot s^{m+1}$)
AF-0 h	0.9960 ± 0.0016^a	-1.12 ± 0.01^b	1186.93 ± 103.92^b
AF-24 h	0.9975 ± 0.0007^a	-1.15 ± 0.01^b	1615.92 ± 105.65^a
AF-48 h	0.9960 ± 0.0007^a	-1.13 ± 0.01^b	1279.30 ± 40.92^b
AF-72 h	0.9976 ± 0.0011^a	-1.06 ± 0.04^a	985.30 ± 46.72^c

Values are presented as the mean ± SD ($n = 3$). Different letters within the same column indicate significant differences ($p < 0.05$).

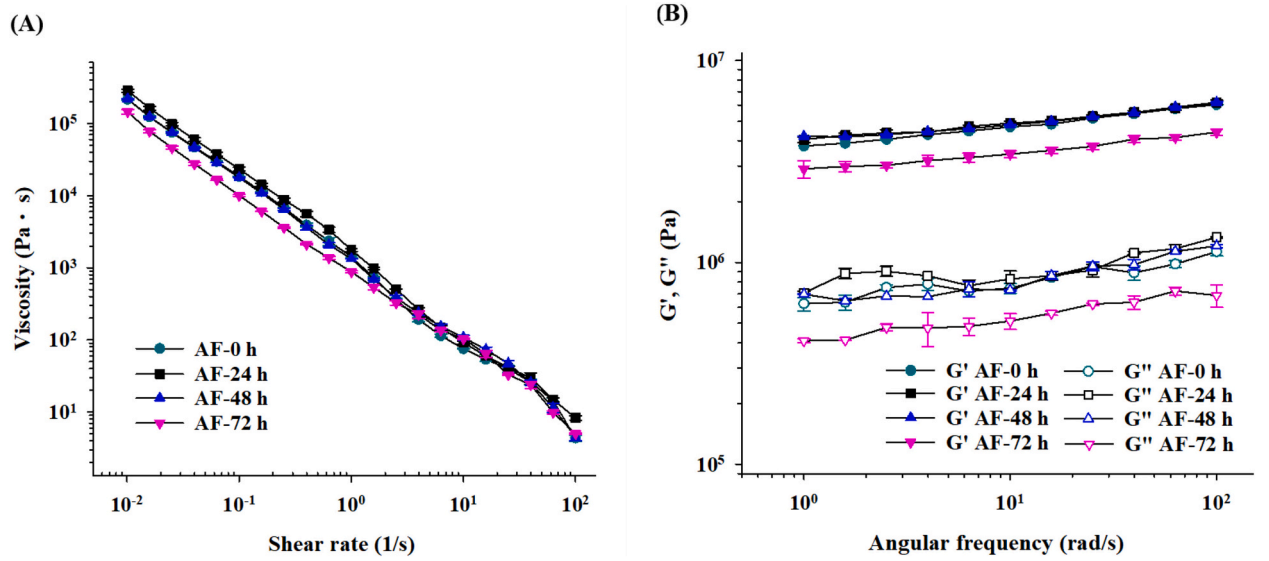


Fig. 5. Viscosity (A) and frequency sweep (B) of artificial fats (AFs) using chickpea powder with different fermentation times.

favorable emulsion performance. Thus, prolonged fermentation was associated with an AF system showing lower resistance to flow and a less developed bulk structure under the present formulation conditions.

The apparent viscosity data were well described by the power-law model, with R^2 values exceeding 0.9960 for all AF systems (Table 5). All AF systems exhibited negative power-law exponents ($m < 0$), confirming the progressive decrease in apparent viscosity with increasing shear rate. The consistency coefficient (K) increased from 1186.93 in AF-0 h to 1615.92 in AF-24 h and subsequently decreased to 1279.30 in AF-48 h and 985.30 in AF-72 h. This trend was consistent with the apparent viscosity profiles, with AF-24 h showing the greatest resistance to flow and AF-72 h the lowest among the tested AF systems. These differences further indicate that fermentation time was associated with changes in the bulk consistency of the coconut oil-based AF systems [42].

Overall, the flow-sweep results indicate that fermentation-associated differences in the chickpea fractions were accompanied by distinct bulk rheological characteristics of the AF systems. Among the tested conditions, AF-24 h exhibited the highest viscosity and consistency coefficient, whereas AF-72 h showed the lowest values. When considered together with the microstructural and emulsion-property results, these findings support an association between the functional state of the chickpea-derived fractions and the rheological organization of the resulting AF systems.

3.3.2. Viscoelastic properties and network characteristics

The viscoelastic properties of the AF systems were evaluated by frequency sweep analysis to characterize their elastic and viscous responses after cooling (Fig. 5B). All AF samples exhibited storage modulus (G′) values consistently higher than loss modulus (G″) throughout the measured angular frequency range, indicating predominantly elastic behavior. The predominance of G′ over G″ is consistent with the formation of weak gel-like or structured emulsion networks rather than purely viscous systems [43].

The magnitude of the viscoelastic response varied among fermentation conditions. AF-24 h exhibited the strongest elastic response, whereas AF-72 h showed the lowest G′ values among the AF systems. The higher G′ of AF-24 h indicates a greater elastic contribution to the bulk structure after cooling and is consistent with its higher apparent viscosity and more homogeneous dispersed microstructure. Conversely, the lower G′ of AF-72 h indicates a weaker elastic response under the present measurement conditions.

These differences were also consistent with the structural and functional characteristics of the corresponding chickpea fractions. AF-24 h was prepared from a fraction exhibiting relatively high protein solubility, H_o, and calculated S—S content and showed favorable emulsion-related characteristics, including a greater absolute zeta potential and higher apparent emulsion activity. These combined properties may have contributed to the formation of a more elastically responsive dispersed structure. Disulfide-associated interactions have been reported to contribute to the rheological properties of protein-containing emulsion systems [44,45]; however, the present measurements do not directly distinguish the contributions of interfacial protein interactions, droplet–droplet interactions, and lipid crystallization to the measured viscoelastic response.

In contrast, the lower G′ of AF-72 h coincided with reduced protein solubility, lower H_o and calculated S—S content, a less homogeneous droplet distribution, and less favorable emulsion performance. These observations suggest that the functional state of the chickpea fraction under prolonged fermentation conditions was less favorable for the development of an elastic-dominant bulk structure after cooling.

Collectively, the frequency-sweep results demonstrate that all AF systems exhibited predominantly elastic behavior, while the magnitude of the viscoelastic response depended on fermentation condition. AF-24 h showed the greatest elastic response, whereas AF-72 h exhibited the weakest response among the tested systems. Together with the flow-sweep results, these findings indicate that fermentation-associated differences in the chickpea fractions were linked to changes in the bulk rheological organization of the AF systems, although the specific molecular and interfacial mechanisms underlying these differences require direct characterization.

3.4. Crystalline and thermal behavior of the structured artificial fat systems

3.4.1. Crystal polymorphism and structural organization

X-ray diffraction (XRD) analysis was performed to compare the crystalline organization of beef tallow, coconut oil, and the AF systems after cooling (Fig. 6A). Fat crystal polymorphism is an important structural characteristic because differences in crystal packing and polymorphic organization can influence the physical properties of fat-based systems [46]. Based on commonly reported WAXD short-spacing assignments for fat polymorphs, the reflection near 4.6 Å was assigned to β-associated crystalline structures, whereas reflections near 4.2 and 3.8 Å were assigned to β′-associated structures [47]. An additional reflection was observed near 3.6 Å; however, this feature was interpreted cautiously because complex lipid systems may exhibit overlapping reflections arising from different triacylglycerol arrangements or coexisting crystalline phases [48,49].

The diffraction profiles differed among beef tallow, coconut oil, and the AF systems. Beef tallow exhibited a distinct crystalline profile containing β-associated features, whereas coconut oil showed a different short-spacing pattern, reflecting differences in lipid composition and crystallization behavior. The AF systems retained major diffraction features associated with coconut oil, but differences in the relative intensity and shape of the reflections were observed following emulsification and cooling. These changes indicate that incorporation of the chickpea-derived aqueous phase and formation of the dispersed AF structure altered the crystallization environment of the coconut oil phase.

Differences were also observed among AF systems prepared with chickpea fractions obtained at different fermentation times. Compared with AF-0 h, the fermented samples showed distinguishable changes in the relative profiles of β- and β′-associated reflections. These differences were consistent with variations in droplet organization and bulk structural characteristics observed among the AF systems. However, because the XRD patterns were obtained from complex emulsified systems and were evaluated as relative diffraction profiles, they were interpreted as qualitative differences in crystalline organization rather than quantitative differences in the proportions of β and β′ polymorphs.

The presence of β′-associated reflections in the AF systems is relevant because β′-type crystalline organization is generally associated with relatively fine crystal structures in fat-based systems, whereas β-type crystals are commonly associated with more stable and coarser crystalline structures [32,50]. Nevertheless, the present XRD data do not establish that the AF systems reproduced the crystalline architecture of beef tallow. Rather, the AF systems developed distinct crystalline profiles derived primarily from the coconut oil phase under the present emulsification and cooling conditions.

Overall, the XRD results indicate that formation of the AF systems was accompanied by changes in the crystalline organization of the dispersed coconut oil phase. Fermentation-associated differences in the chickpea-derived fractions were also accompanied by differences in the relative diffraction profiles of the resulting AF systems. These findings support an association between the structural characteristics of the AF systems and their lipid-phase organization, although the specific mechanisms by which the protein-containing interfacial environment influences crystallization were not directly determined.

3.4.2. Crystallization and melting transitions

Differential scanning calorimetry (DSC) was used to compare the crystallization and melting transitions of beef tallow, coconut oil, and the AF systems (Figs. 6B and 6C). During cooling, beef tallow exhibited

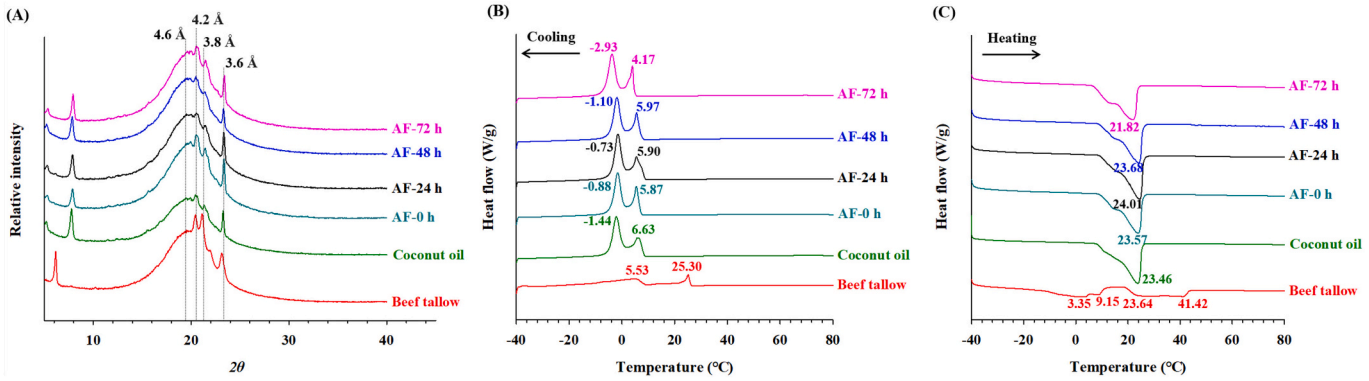


Fig. 6. XRD patterns (A), crystallization thermogram (B), and melting thermogram (C) of beef tallow, coconut oil, and artificial fats (AFs) using chickpea powders with different fermentation times.

crystallization peaks at 5.53 and 25.30 °C, reflecting crystallization of different lipid fractions. In contrast, coconut oil showed crystallization transitions at −1.44 and 6.63 °C. These differences are consistent with the distinct fatty acid and triacylglycerol compositions of animal fat and coconut oil [46].

The AF systems also exhibited two crystallization transitions during cooling. The higher-temperature crystallization peaks of AF-0 h, AF-24 h, AF-48 h, and AF-72 h occurred at 5.87, 5.90, 5.97, and 4.17 °C, respectively, while the lower-temperature transitions occurred at −0.88, −0.73, −1.10, and − 2.93 °C, respectively. Compared with pure coconut oil, these shifts indicate that emulsification and formation of the AF structure altered the thermal crystallization behavior of the dispersed coconut oil phase. In dispersed lipid systems, crystallization can be affected by droplet organization, interfacial composition, and spatial confinement of the lipid phase [51]. Accordingly, the observed transition shifts are consistent with changes in the crystallization environment created by the AF formulation rather than changes in the intrinsic composition of coconut oil itself.

The fermentation-dependent differences in crystallization transitions were non-linear. AF-0 h, AF-24 h, and AF-48 h showed relatively similar higher-temperature crystallization peaks, whereas AF-72 h exhibited the lowest transition temperature at 4.17 °C and also the lowest lower-temperature transition at −2.93 °C. This downward shift coincided with the lower protein solubility, H_0, and calculated S—S content of the corresponding chickpea fraction, as well as the less homogeneous droplet structure and weaker bulk rheological response observed for AF-72 h. These concurrent changes suggest that the structural environment of AF-72 h was less favorable for crystallization at higher temperatures; however, the present data do not allow the individual contributions of protein structure, interfacial organization, droplet confinement, and lipid–protein interactions to be separated.

The melting thermograms also differed among beef tallow, coconut oil, and the AF systems (Fig. 6C). Beef tallow exhibited multiple endothermic peaks at 3.35, 9.15, 23.64, and 41.42 °C, reflecting the melting of multiple triacylglycerol fractions and crystalline populations [32]. In contrast, coconut oil and the AF systems exhibited broader major melting transitions. The major melting peak of coconut oil occurred at 23.46 °C, whereas those of AF-0 h, AF-24 h, AF-48 h, and AF-72 h occurred at 23.57, 24.01, 23.68, and 21.82 °C, respectively.

The melting transitions did not change linearly with fermentation time. AF-24 h showed a slightly higher major melting peak than coconut oil and AF-0 h, whereas AF-72 h exhibited the lowest melting peak among the AF systems. These thermal differences were consistent with the fermentation-dependent differences observed in microstructure, emulsion performance, rheological behavior, and XRD profiles. In particular, the lower melting transition of AF-72 h was accompanied by its less favorable dispersed and bulk structural characteristics. Therefore, the DSC results indicate that the thermal behavior of the coconut oil phase differed among AF systems prepared with chickpea fractions obtained at different fermentation times, without implying a direct causal effect of a specific protein structural change on lipid melting behavior.

Collectively, the DSC and XRD results show that incorporation of chickpea-derived fractions into coconut oil-based AF systems produced crystalline and thermal characteristics distinct from those of pure coconut oil. Differences among fermentation conditions were also observed, with AF-24 h generally exhibiting structural and thermal characteristics consistent with a more organized AF system, whereas AF-72 h showed lower crystallization and melting transition temperatures together with less favorable microstructural and rheological characteristics. These findings indicate that fermentation-associated differences in the chickpea fractions were linked to the lipid-phase organization of the resulting AF systems, while the underlying crystallization mechanisms require further direct investigation.

Color and volatile profiles are presented in Tables S2 and S3 as supplementary information on sensory-related attributes, whereas the structure-function relationship of the coconut oil-based AF systems was primarily interpreted based on protein structural, interfacial, rheological, crystalline, and thermal analyses.

4. Conclusion

This study demonstrated fermentation-associated changes in the structural and functional characteristics of chickpea-derived protein fractions and their relationship with the performance of coconut oil-based artificial fat (AF) systems. Increasing fermentation time was accompanied by changes in protein molecular profiles, secondary structure, thiol–disulfide balance, solubility, and surface hydrophobicity. Among the tested conditions, 24 h fermentation provided the most favorable combination of protein solubility and surface hydrophobicity, together with relatively high calculated disulfide-associated bonding. When incorporated into AF systems, the 24 h fermented chickpea fraction was associated with more homogeneous droplet organization, greater absolute zeta potential, higher apparent emulsion activity, greater thermal retention of emulsion activity, and stronger bulk rheological responses. XRD and DSC analyses further showed that the AF systems exhibited crystalline and thermal characteristics distinct from pure coconut oil, with fermentation-dependent differences in lipid-phase organization and crystallization–melting behavior. In contrast, the 72 h fermented fraction showed lower protein dispersibility and less favorable emulsion, rheological, and lipid-phase characteristics. Overall, these findings indicate that controlled *R. oryzae* fermentation can be used to modify the functional state of chickpea-derived fractions and is associated with changes in the structural performance of coconut oil-based AF systems. The results support the potential of fermentation-modified chickpea fractions as plant-derived structuring components

for artificial fat applications. Further studies incorporating direct interfacial characterization, droplet-size analysis, processing performance, and sensory evaluation are needed to clarify the mechanisms underlying these structure–function relationships and to assess their practical applicability in food systems.

CRediT authorship contribution statement

Jung Soo Kim: Writing – review & editing, Writing – original draft, Validation, Project administration, Methodology, Investigation, Funding acquisition, Formal analysis, Conceptualization. **Jiyoon Kim:** Writing – review & editing, Writing – original draft, Visualization, Validation, Methodology, Investigation, Formal analysis, Data curation. **Kwang-Deog Moon:** Supervision, Resources.

Declaration of competing interest

The authors declare that they have no known competing financial interests or personal relationships that could have appeared to influence the work reported in this paper.

Acknowledgments

This work was supported by Basic Science Research Program through the National Research Foundation of Korea (NRF) funded by the Ministry of Education [grant number RS-2023-00273056].

Appendix A. Supplementary data

Supplementary data to this article can be found online at https://doi.org/10.1016/j.ijbiomac.2026.155000.

Data availability

Data will be made available on request.

References

[1] A. Mookerjee, T. Tanaka, Influence of enzymatic treatments on legume proteins for improved functional and nutritional properties: expansion of legume protein utilization as food ingredients, Curr. Opin. Food Sci. 49 (2023) 100974, https://doi.org/10.1016/J.COFS.2022.100974.
[2] J. Lee, H. Song, K.H. Seo, H.G. Lee, H. Kim, M.J. Choi, Physicochemical and sensory properties of plant-based meat patties using oil-in-water emulsion, Food Biosci. 56 (2023) 103084, https://doi.org/10.1016/J.FBIO.2023.103084.
[3] V. Syan, J. Kaur, K. Sharma, M. Patni, P. Rasane, J. Singh, V. Bhadariya, An overview on the types, applications and health implications of fat replacers, J. Food Sci. Technol. 61 (2024) 27–38, https://doi.org/10.1007/S13197-022-05642-7.
[4] Y.J. Ng, P.E. Tham, K.S. Khoo, C.K. Cheng, K.W. Chew, P.L. Show, A comprehensive review on the techniques for coconut oil extraction and its application, Bioprocess Biosyst. Eng. 44 (2021) 1807–1818, https://doi.org/10.1007/S00449-021-02577-9.
[5] Y. Liu, Q. Wu, J. Zhang, W. Yan, X. Mao, Food emulsions stabilized by proteins and emulsifiers: a review of the mechanistic explorations, Int. J. Biol. Macromol. 261 (2024) 129795, https://doi.org/10.1016/J.IJBIOMAC.2024.129795.
[6] R.R. Lima, R. Stephani, Í.T. Perrone, A.F. de Carvalho, Plant-based proteins: a review of factors modifying the protein structure and affecting emulsifying properties, Food Chem. Adv. 3 (2023) 100397, https://doi.org/10.1016/J.FOCHA.2023.100397.
[7] Y. Liu, X. Guo, T. Liu, X. Fan, X. Yu, J. Zhang, Study on the structural characteristics and emulsifying properties of chickpea protein isolate-citrus pectin conjugates prepared by Maillard reaction, Int. J. Biol. Macromol. 264 (2024) 130606, https://doi.org/10.1016/j.ijbiomac.2024.130606.
[8] L.M. Sánchez-Magaña, E.O. Cuevas-Rodríguez, R. Gutiérrez-Dorado, A.E. Ayala-Rodríguez, A. Valdez-Ortiz, J. Milán-Carrillo, C. Reyes-Moreno, Solid-state bioconversion of chickpea (*Cicer arietinum* L.) by Rhizopus oligosporus to improve total phenolic content, antioxidant activity and hypoglycemic functionality, Int. J. Food Sci. Nutr. 65 (2014) 558–564, https://doi.org/10.3109/09637486.2014.893284.
[9] Y. Liu, S. Zhu, Y. Li, F. Sun, D. Huang, X. Chen, Alternations in the multilevel structures of chickpea protein during fermentation and their relationship with digestibility, Food Res. Int. 165 (2023) 112453, https://doi.org/10.1016/J.FOODRES.2022.112453.
[10] I.D. Okehie, M.N. Riza, S. Pillai, R. Ovissipour, Enhanced nutritional quality, digestibility, and flavor of grasshopper through solid state fermentation, Sci. Rep. 16 (2026) 10918, https://doi.org/10.1038/s41598-026-45428-x.
[11] Q. Du, H. Li, M. Tu, Z. Wu, T. Zhang, J. Liu, Y. Ding, X. Zeng, D. Pan, Legume protein fermented by lactic acid bacteria: specific enzymatic hydrolysis, protein composition, structure, and functional properties, Colloids Surf. B: Biointerfaces 238 (2024) 113929, https://doi.org/10.1016/J.COLSURFB.2024.113929.
[12] N. Grasso, N.L. Lynch, E.K. Arendt, J.A. O'Mahony, Chickpea protein ingredients: a review of composition, functionality, and applications, Compr. Rev. Food Sci. Food Saf. 21 (2022) 435–452, https://doi.org/10.1111/1541-4337.12878.
[13] S.B. Erkan, H.N. Gürler, D.G. Bilgin, M. Germec, I. Turhan, Production and characterization of tempehs from different sources of legume by *Rhizopus oligosporus*, LWT 119 (2020) 108880, https://doi.org/10.1016/j.lwt.2019.108880.
[14] C. Reyes-Moreno, C. Romero-Urías, J. Milán-Carrillo, B. Valdéz-Torres, E. Zárate-Márquez, Optimization of the solid state fermentation process to obtain tempeh from hardened chickpeas (*Cicer arietinum* L.), Plant Foods Hum. Nutr. 55 (2000) 219–228, https://doi.org/10.1023/A:1008190918425.
[15] J.S. Kim, J. Kim, S.H. Kim, K.D. Moon, Development of chickpea tempeh using *Rhizopus oryzae* for dysphagia diet: effect of fermentation time and heat treatment, Innov. Food Sci. Emerg. Technol. 100 (2025) 103940, https://doi.org/10.1016/j.ifset.2025.103940.
[16] Y. Ma, J. Zhang, J. He, Y. Xu, X. Guo, Effects of high-pressure homogenization on the physicochemical, foaming, and emulsifying properties of chickpea protein, Food Res. Int. 170 (2023) 112986, https://doi.org/10.1016/J.FOODRES.2023.112986.
[17] Y. Hu, H. Chen, Y. Yang, S. Zhang, Z. Xie, J. Liu, Q. Jiang, J. Liu, P. Wen, Comparison of ovalbumin glycation induced by high-temperature steaming and high-temperature baking: a study combining conventional spectroscopy with high-resolution mass spectrometry, Food Res. Int. 173 (2023) 113279, https://doi.org/10.1016/J.FOODRES.2023.113279.
[18] M. Tan, J. Xu, H. Gao, Z. Yu, J. Liang, D. Mu, X. Li, X. Zhong, S. Luo, Y. Zhao, S. Jiang, Z. Zheng, Effects of combined high hydrostatic pressure and pH-shifting pretreatment on the structure and emulsifying properties of soy protein isolates, J. Food Eng. 306 (2021) 110622, https://doi.org/10.1016/J.JFOODENG.2021.110622.
[19] R. Wang, L.H. Wang, Q.H. Wen, F. He, F.Y. Xu, B.R. Chen, X.A. Zeng, Combination of pulsed electric field and pH shifting improves the solubility, emulsifying, foaming of commercial soy protein isolate, Food Hydrocoll. 134 (2023) 108049, https://doi.org/10.1016/J.FOODHYD.2022.108049.
[20] M. Satapathy, D. Quereshi, T.T. Hanh Nguyen, D. Pani, B. Mohanty, A. Anis, S. Maji, D. Kim, P. Sarkar, K. Pal, Preparation and characterization of cocoa butter and whey protein isolate based emulgels for pharmaceutical and probiotics delivery applications, J. Dispers. Sci. Technol. 41 (2020) 426–440, https://doi.org/10.1080/01932691.2019.1583577.
[21] N. Li, T. Wang, X. Yang, J. Qu, N. Wang, L. Wang, D. Yu, C. Han, Effect of high-intensity ultrasonic treatment on the emulsion of hemp seed oil stabilized with hemp seed protein, Ultrason. Sonochem. 86 (2022) 106021, https://doi.org/10.1016/J.ULTSONCH.2022.106021.
[22] H. Du, J. Zhang, S. Wang, A. Manyande, J. Wang, Effect of high-intensity ultrasonic treatment on the physicochemical, structural, rheological, behavioral, and foaming properties of pumpkin (*Cucurbita moschata* Duch.)-seed protein isolates, LWT 155 (2022) 112952, https://doi.org/10.1016/J.LWT.2021.112952.
[23] X. Yang, C. Ke, L. Li, Physicochemical, rheological and digestive characteristics of soy protein isolate gel induced by lactic acid bacteria, J. Food Eng. 292 (2021) 110243, https://doi.org/10.1016/J.JFOODENG.2020.110243.
[24] Y. Bai, Z. Zhang, J. Qiao, Y.Q. Liang, P. Yang, S. Zhao, G. Ren, L. Zhang, Impact of Lactobacillus plantarum fermentation on the structural, physicochemical, emulsification, and digestibility properties of foxtail millet protein, Food Chem. 482 (2025) 144141, https://doi.org/10.1016/J.FOODCHEM.2025.144141.
[25] Z. Zheng, J. Li, J. Li, H. Sun, Y. Liu, Physicochemical and antioxidative characteristics of black bean protein hydrolysates obtained from different enzymes, Food Hydrocoll. 97 (2019) 105222, https://doi.org/10.1016/J.FOODHYD.2019.105222.
[26] X. Jia, L. Li, J.W. Teng, M. Li, H. Long, N. Xia, Glycation of rice protein and D-xylose pretreated through hydrothermal cooking-assisted high hydrostatic pressure: focus on the structural and functional properties, LWT 160 (2022) 113194, https://doi.org/10.1016/J.LWT.2022.113194.
[27] D. Peng, W. Huang, H. Bao, W. Ding, X. Pan, G. Li, L. Dong, W. Li, J. Chen, P. Li, B. Du, Glucose-induced glycation enhances the foaming properties of Trichosanthes kirilowii seed protein isolate: insights into structure, interfacial behavior, and proteomics, Food Hydrocoll. 157 (2024) 110444, https://doi.org/10.1016/J.FOODHYD.2024.110444.
[28] R. Wang, Y. Ma, Z. Ma, Q. Du, Y. Zhao, Y. Chi, Changes in gelation, aggregation and intermolecular forces in frozen-thawed egg yolks during freezing, Food Hydrocoll. 108 (2020) 105947, https://doi.org/10.1016/J.FOODHYD.2020.105947.
[29] M. Yu, M. Zeng, F. Qin, Z. He, J. Chen, Physicochemical and functional properties of protein extracts from Torreya grandis seeds, Food Chem. 227 (2017) 453–460, https://doi.org/10.1016/J.FOODCHEM.2017.01.114.
[30] Y. Xiao, G. Xing, X. Rui, W. Li, X. Chen, M. Jiang, M. Dong, Effect of solid-state fermentation with *Cordyceps militaris* SN-18 on physicochemical and functional properties of chickpea (*Cicer arietinum* L.) flour, LWT 63 (2015) 1317–1324, https://doi.org/10.1016/J.LWT.2015.04.046.
[31] Y. Wang, Y. Wang, K. Li, Y. Bai, B. Li, W. Xu, Effect of high intensity ultrasound on physicochemical, interfacial and gel properties of chickpea protein isolate, LWT 129 (2020) 109563, https://doi.org/10.1016/J.LWT.2020.109563.

[32] Z. Zeng, X. Qin, H. Wang, Z. Chen, D. Huang, D. Xiang, X. Liu, Effect of the chemical composition and structural properties of beef tallow from different adipose tissues on bread quality, LWT 192 (2024) 115736, https://doi.org/10.1016/J.LWT.2024.115736.
[33] Y. Wang, R. Wang, Y. Li, L. Zhang, Beef tallow/lard blends in O/W emulsions: characterization of fat crystals, partial coalescence, rheology, and aeration performance, Food Res. Int. 172 (2023) 113140, https://doi.org/10.1016/J.FOODRES.2023.113140.
[34] K. Chaleepa, A. Szepes, J. Ulrich, Effect of additives on isothermal crystallization kinetics and physical characteristics of coconut oil, Chem. Phys. Lipids 163 (2010) 390–396, https://doi.org/10.1016/J.CHEMPHYSLIP.2010.03.005.
[35] Z. Kang, S. Zhang, Y. Kong, Z. Wu, Y. Li, T. Liu, F. Xie, Modification of soybean protein isolate by pH-shifting combined with ultrasonic treatment: structural, viscosity, and functional properties, Food Struct. 42 (2024) 100383, https://doi.org/10.1016/J.FOOSTR.2024.100383.
[36] M. Zhang, L. Fan, Y. Liu, S. Huang, J. Li, Effects of proteins on emulsion stability: the role of proteins at the oil–water interface, Food Chem. 397 (2022) 133726, https://doi.org/10.1016/J.FOODCHEM.2022.133726.
[37] Y. Liu, X. Fan, X. Yu, T. Liu, J. Zhang, Improving the emulsifying properties and oil–water interfacial behaviors of chickpea protein isolates through Maillard reaction with citrus pectin, Int. J. Biol. Macromol. 283 (2024) 137671, https://doi.org/10.1016/j.ijbiomac.2024.137671.
[38] X. Zhang, Y. Chen, R. Li, Y. Shi, Y. Zhao, B. Li, Y. Chen, X. Zhu, Fabrication of pea protein isolate-stabilized oil-in-water emulsions with high freeze-thaw stability: effect of high intensity ultrasonic on emulsions and interfacial protein structure, Food Hydrocoll. 157 (2024) 110484, https://doi.org/10.1016/J.FOODHYD.2024.110484.
[39] Z. Cai, Y. Wei, A. Shi, J. Zhong, P. Rao, Q. Wang, H. Zhang, Correlation between interfacial layer properties and physical stability of food emulsions: current trends, challenges, strategies, and further perspectives, Adv. Colloid Interf. Sci. 313 (2023) 102863, https://doi.org/10.1016/J.CIS.2023.102863.
[40] E.B. Heggset, R. Aaen, T. Veslum, M. Henriksson, S. Simon, K. Syverud, Cellulose nanofibrils as rheology modifier in mayonnaise – a pilot scale demonstration, Food Hydrocoll. 108 (2020) 106084, https://doi.org/10.1016/J.FOODHYD.2020.106084.
[41] Y. Kumar, S. Roy, A. Devra, A. Dhiman, P.K. Prabhakar, Ultrasonication of mayonnaise formulated with xanthan and guar gums: rheological modeling, effects on optical properties and emulsion stability, LWT 149 (2021) 111632, https://doi.org/10.1016/J.LWT.2021.111632.
[42] J. Techarang, A. Apichartsrangkoon, Physical, chemical and rheological parameters of pressurized swai-fish (*Pangasius hypophthalmus*) emulsion incorporating fermented soybeans, Food Bioprod. Process. 94 (2015) 649–656, https://doi.org/10.1016/J.FBP.2014.09.002.
[43] I. Alouk, W. Lv, W. Chen, S. Miao, C. Chen, Y. Wang, D. Xu, Encapsulation of Monascus pigments in gel in oil in water (G/O/W) double emulsion system based on sodium caseinate and guar gum, Int. J. Biol. Macromol. 285 (2025) 138232, https://doi.org/10.1016/j.ijbiomac.2024.138232.
[44] B. Chen, X. Liu, K. Zhou, Y. Xie, Y. Wang, H. Zhou, Y. Bai, B. Xu, Differentiating the effects of hydrophobic interaction and disulfide bond on the myofibrillar protein emulsion gels at the high temperature and the protein interfacial properties, Food Chem. 412 (2023) 135472, https://doi.org/10.1016/J.FOODCHEM.2023.135472.
[45] Y. Wang, N.N. Liu, K. Li, B. Chen, J.L. Wang, J.G. Li, Y.H. Bai, Assessing how the partial substitution of phosphate by modified chickpea protein affects the technofunctional, rheological, and structural characteristics of pork meat emulsions, Meat Sci. 225 (2025) 109812, https://doi.org/10.1016/j.meatsci.2025.109812.
[46] J. Mao, Y. Gao, Z. Meng, Crystallization behavior and compatibility analysis of beef tallow-based binary/ternary fat mixture systems, Food Res. Int. 161 (2022) 111814, https://doi.org/10.1016/J.FOODRES.2022.111814.
[47] C. Lopez, C. Bourgaux, P. Lesieur, M. Ollivon, Crystalline structures formed in cream and anhydrous milk fat at 4°C, Lait 82 (2002) 317–335, https://doi.org/10.1051/lait:2002013.
[48] X. Hong, Q. Zhao, J. Chen, T. Ye, L. Fan, J. Li, Fabrication and characterization of oleogels and temperature-responsive water-in-oil emulsions based on candelilla (*Euphorbia cerifera*) wax, Food Chem. 397 (2022) 133677, https://doi.org/10.1016/j.foodchem.2022.133677.
[49] L. Li, G. Liu, Engineering effect of oleogels with different structuring mechanisms on the crystallization behavior of cocoa butter, Food Chem. 422 (2023) 136292, https://doi.org/10.1016/j.foodchem.2023.136292.
[50] C. Liu, Z. Meng, P. Cao, J. Jiang, X. Liang, M. Piatko, S. Campbell, S.K. Lo, Y. Liu, Visualized phase behavior of binary blends of coconut oil and palm stearin, Food Chem. 266 (2018) 66–72, https://doi.org/10.1016/J.FOODCHEM.2018.05.118.
[51] J. Cheng, Q. Kan, J. Cao, O.E. Dudu, T. Yan, Interfacial compositions of fat globules modulate coconut oil crystallization behavior and stability of whipped-frozen emulsions, Food Hydrocoll. 114 (2021) 106580, https://doi.org/10.1016/j.foodhyd.2020.106580.